Research Square

Preprints are preliminary reports that have not undergone peer review.
They should not be considered conclusive, used to inform clinical practice,
or referenced by the media as validated information.

Urban expansion, seasonal climate and fine particulate matter in Lahore, Pakistan: a spatiotemporal analysis of regional environmental change (2015–2024)

Saqib rehman

saqib.rehman@uok.edu.pk

University of Karachi

Bilal Usmani

Aga Khan University

Shumaila Naz

University of Karachi

zafar Ahmed

Aga Khan University

zafar fatmi

Aga Khan University

Research Article

Keywords: Urbanization, Land-use change, Climate variability, Spatial non-stationarity, Indo-Gangetic Plain, Lahore

Posted Date: November 5th, 2026

DOI: https://doi.org/10.21203/rs.3.rs-11602212/v1

License: This work is licensed under a Creative Commons Attribution 4.0 International License.
Read Full License

Additional Declarations: No competing interests reported.

Urban expansion, seasonal climate and fine particulate matter in Lahore, Pakistan: a spatiotemporal analysis of regional environmental change (2015–2024)

Saqib Ur Rehman[1]*, Bilal Usmani[2], Shumaila Naz[1], Zafar Ahmed[3], Zafar Fatmi[4]

*[1]Department of Mathematics, University of Karachi, Pakistan. *Corresponding author*

City: Karachi

[2]Epidemiology and Biostatistics Section, Department of Community Health Sciences, Medical College, Aga Khan University, Pakistan

City: Karachi

[3]Department of Social Work, Education and Community Wellbeing, Northumbria University, UK

City: Newcastle Upon Tyne

[4]Section of Environmental-Occupational Health & Climate Change, Department of Community Health Sciences, Aga Khan University, Pakistan

City: Karachi

**saqib.rehman@uok.edu.pk; bilal.usmani@aku.edu; shumanaz27@gmail.com;*

zafar.ahmed@northumbria.ac.uk; zafar.fatmi@aku.edu

Abstract

Background: Rapid urban expansion and land-use change in the Indo-Gangetic Plain interact with seasonal climate to shape regional air quality, yet how associations of fine particulate matter ($PM_{2.5}$) with climatic and urban-growth factors vary jointly across space and time within one urban region is poorly understood. This study examined these associations across Lahore, Pakistan.

Methods: Satellite-derived $PM_{2.5}$ (2015–2024) was analysed using two geographically and temporally weighted regression (GTWR) models: a climatic model (temperature, relative humidity, rainfall and wind speed; 1,400 point-seasons) and a socioeconomic model (built-up area, road density and population; 5,710 point-years). Local coefficients significant at the 5% level ($|t| \geq 1.96$) were mapped.

Results: Annual mean $PM_{2.5}$ ranged from 62.9 to 74.5 µg/m³, increased modestly (about 4.7% over the decade), spread from the centre toward the periphery and peaked in winter. In the climatic model ($R^2 = 0.894$), relative humidity was positively and rainfall negatively associated with $PM_{2.5}$, temperature was predominantly negative, and wind speed changed sign: dispersive in the open north-east but positive in the western fringe, consistent with transport of regional crop-burning smoke. In the socioeconomic model ($R^2 = 0.562$), built-up area, road density and population were predominantly positive drivers, strongest on the rapidly urbanizing south-western periphery and in the congested Youhanabad/Model Town corridor.

Conclusions: $PM_{2.5}$ in Lahore reflects a structural urban baseline overlaid by a strongly seasonal climatic signal. Converging climatic and structural hotspots on the south-western fringe call for spatially and seasonally differentiated interventions.

Keywords: Urbanization; Land-use change; Climate variability; Spatial non-stationarity; Indo-Gangetic Plain; Lahore

1. Introduction

Fine particulate matter ($PM_{2.5}$; particles with an aerodynamic diameter ≤2.5 μm) is the leading environmental risk factor globally, contributing to premature mortality from cardiovascular and respiratory disease, stroke and lung cancer (Hamra et al. 2014; Cohen et al. 2017; Vodonos et al. 2018; Murray et al. 2020; Alexeeff et al. 2021; Southerland et al. 2022). Because these particles penetrate deep into the lungs and can enter the bloodstream, long-term exposure is associated with higher risks of ischaemic heart disease, stroke and lung cancer, and meta-analyses report associations with mortality across a wide range of concentrations (Hamra et al. 2014; Vodonos et al. 2018; Alexeeff et al. 2021). Ambient air pollution caused approximately 4.2 million premature deaths in 2019, nearly half of them in urban areas, where more than 55% of the world's population lives and where this share is expected to reach about 60% by 2030 (Cohen et al. 2017; United Nations 2018; Southerland et al. 2022). The burden is heaviest in rapidly urbanizing low- and middle-income countries, where most urban residents live in areas that exceed health-based guidelines and where growing urban populations increase the number of people exposed (Southerland et al. 2022).

$PM_{2.5}$ also affects the Earth's radiation balance, while meteorological conditions regulate its formation, transport, dispersion and removal (UNEP 2021); understanding its controlling factors is therefore central to both air-quality management and climate adaptation (United Nations 1992). $PM_{2.5}$ is a mixture of primary particles, emitted directly by combustion, industry and dust, and secondary particles formed in the atmosphere from precursor gases. Its concentration at any place therefore reflects both local emissions and atmospheric processes acting over hours to days. Effective management requires knowing not only where emissions originate but also under which conditions they accumulate.

Urbanization, industrialization, transport and land-use change are well-established anthropogenic drivers of $PM_{2.5}$ (Molina and Molina 2004; Gurjar et al. 2008; Fernando et al. 2012; Siwek and Osowski 2012; He et al. 2017; Luo et al. 2018; Wang et al. 2018, 2020; Chen et al. 2019). In megacities, dense traffic, energy use, construction and industrial activity concentrate emissions in a small area (Molina and Molina 2004; Gurjar et al. 2008), and studies of Chinese cities and cross-country panels have linked $PM_{2.5}$ to urban expansion, population growth, economic structure and technological change (Luo et al. 2018; Wang et al. 2018, 2020; Chen et al. 2019). At the same time, temperature, wind speed, humidity and precipitation modulate $PM_{2.5}$ through their effects on atmospheric stability, chemistry and dispersion (Zhan et al. 2018; Liu et al. 2020). Stagnant, humid conditions with shallow boundary layers favour accumulation and secondary aerosol formation, whereas wind and rain disperse and remove particles (He et al. 2017; Zhan et al. 2018). Their relative contributions, however, vary across space and time, particularly in rapidly growing cities,

where land use, emission sources and local meteorology change over short distances and from season to season.

Commonly used approaches, including linear regression, generalized additive models, Stochastic Impacts by Regression on Population, Affluence and Technology (STIRPAT) models, geographical detector models and positive matrix factorization (Lecoeur and Seigneur 2013; Bari and Kindzierski 2017; Wang et al. 2017, 2018; Luo et al. 2018; Zhan et al. 2018), generally assume spatial or temporal stationarity, treat climatic and socioeconomic factors separately, or rely on data of limited spatial or temporal resolution (Liu 2013; Megaritis et al. 2014; Lyu et al. 2016; Cheng et al. 2017; Liu et al. 2019; Wang et al. 2019). Global regression models estimate a single coefficient for each factor across the whole study area, so opposing local effects can cancel out and produce weak or misleading average relationships. Source-apportionment and chemical-transport studies, although valuable, are usually limited to a few sites or periods (Lecoeur and Seigneur 2013; Megaritis et al. 2014; Bari and Kindzierski 2017). Geographically weighted regression relaxes the assumption of spatial stationarity by estimating local coefficients, and geographically and temporally weighted regression (GTWR) extends this by allowing regression coefficients to vary over both location and time (Huang et al. 2010). GTWR has shown that the effects of socioeconomic and natural factors on $PM_{2.5}$ differ markedly between places and years (Liu et al. 2020). However, most studies of the drivers of $PM_{2.5}$, including GTWR applications, have been conducted at national or regional scale using city- or country-level averages (Cheng et al. 2017; Liu et al. 2019, 2020; Wang et al. 2019), and city-scale applications that can inform local management remain scarce.

Air quality in rapidly growing cities is increasingly an expression of regional environmental change rather than of local emissions alone. Across South Asia, cities are expanding into surrounding agricultural land, converting cropland to built-up area and extending road networks into their hinterlands, while seasonal climate, including winter stagnation and monsoon rainfall, governs how the resulting emissions accumulate or disperse (Molina and Molina 2004; Gurjar et al. 2008; Zhan et al. 2018). In the Indo-Gangetic Plain, these processes interact with trans-boundary influences, such as seasonal crop-residue burning across the Pakistan–India border, so that $PM_{2.5}$ in any one city reflects land-use change, climate and cross-jurisdictional sources together (Ali and Athar 2010; Bilal et al. 2022). Understanding where and when urban growth and climate are most strongly associated with $PM_{2.5}$ therefore helps identify which parts of an expanding urban region, and which seasons, are most vulnerable, and provides evidence relevant to other megacities of the Indo-Gangetic Plain that face similar pressures.

Lahore, Pakistan's second-largest city, consistently ranks among the world's most polluted cities and experiences severe winter smog (Ali and Athar 2010; Khanum et al. 2017; Bilal et al. 2022). Located in the north-western Indo-Gangetic Plain, the city combines a growing population, expanding road traffic and industry with winter conditions that trap pollutants near the surface: low wind speeds, temperature inversions, high humidity and fog (Khanum et al. 2017; Bilal et al. 2022). Its poor air quality has been linked to transport, industry, biomass burning and transboundary pollution (Aziz and Bajwa 2007, 2008; Ali and Athar 2010; Khanum et al. 2017; Bilal et al. 2022), with documented cardiovascular and respiratory health effects (Sughis et al. 2012; Mehmood et al. 2021b) and a mitigating role of urban vegetation (Khan et al. 2022). Studies in the city have

reported higher blood pressure in schoolchildren exposed to particulate pollution (Sughis et al. 2012) and increased hospital admissions associated with air pollution (Mehmood et al. 2021b). Most studies, however, have relied on short-term monitoring at a few sites or examined individual sources, and the long-term spatiotemporal interplay of climatic and socioeconomic drivers across the city is not known. Satellite-derived $PM_{2.5}$ estimates and reanalysis meteorology now make it possible to examine this interplay continuously over space and time in cities where ground monitoring is sparse.

This study applies GTWR to Lahore for 2015–2024 to (i) characterize the spatial and temporal variation of $PM_{2.5}$, (ii) quantify the local effects of temperature, relative humidity, rainfall and wind speed, and (iii) quantify the local effects of built-up area, road density and population, in order to inform land-use planning and regional adaptation in rapidly urbanizing regions. By combining a decade of satellite-derived $PM_{2.5}$, reanalysis meteorology and remote-sensing-based indicators of urban growth, the study identifies where and in which seasons each factor is most strongly associated with $PM_{2.5}$, and where climatic and socioeconomic influences coincide. The approach is transferable to other data-limited cities in South Asia.

2. Materials and Methods

2.1 Study Area

Lahore (approximately 31.55°N, 74.34°E), the capital of Punjab province, lies in north-eastern Pakistan on the Ravi River (Fig. 1a). It had a population of about 13.0 million at the 2023 census, up from 11.1 million in 2017, an average increase of about 2.7% per year (Pakistan Bureau of Statistics 2017, 2023), and has a semi-arid climate with cool, foggy winters (late November to mid-February), hot summers (April to June) and monsoon rainfall peaking in July. The city comprises nine towns: Ravi, Shalimar, Data Ganj Bakhsh, Aziz Bhatti, Samanabad, Gulberg, Wagah, Nishtar and Iqbal, together with the Lahore Cantonment (Fig. 1b).

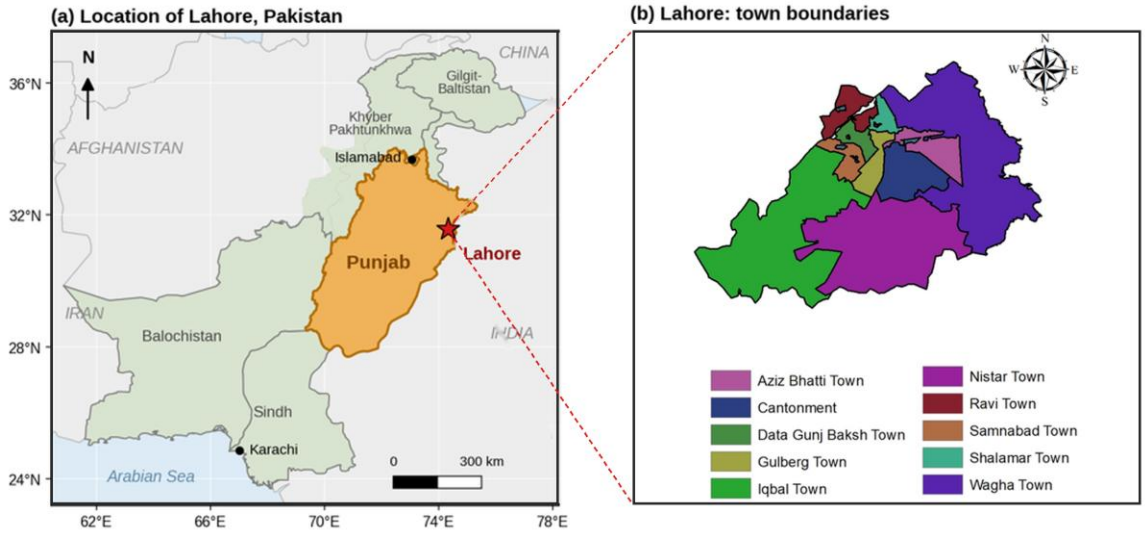


Fig. 1 Study area: (a) location of Lahore in Punjab province, Pakistan; (b) map of Lahore with town boundaries

Lahore is a major industrial and commercial hub, with approximately 4 million registered vehicles and about 2,150 industries, including automobile, steel, chemical, pharmaceutical and construction-material manufacturing, and it contributes about 11.5% of Pakistan's national economy (Tahir 2017). Its main transport corridors include Canal Road, Ring Road, Ferozepur Road, Raiwind Road, Grand Trunk (GT) Road and the M-2, M-3 and M-11 motorways. Industrial and traffic emissions, coal combustion and biomass burning are the principal local sources of air pollution.

2.2 Data

2.2.1 $PM_{2.5}$ Data

Monthly and annual ground-level $PM_{2.5}$ for 2015–2024 were obtained from the V5.GL.06 product of the Atmospheric Composition Analysis Group (ACAG) at Washington University in St. Louis, at 0.01° (≈1 km) resolution. The product combines satellite aerosol optical depth with the GEOS-Chem chemical transport model and is calibrated to ground-based observations by geographically weighted regression (van Donkelaar et al. 2016, 2021). V5.GL.06 applies a single methodology over 1998–2024 with an updated set of calibration monitors; its developers report annual-mean R^2 values against ground monitors of 0.68–0.91 across Asia and have assessed the effect of changes in satellite instruments (van Donkelaar et al. 2021; Hammer et al. 2023; SatPM n.d.).

2.2.2 Meteorological Data

Monthly 2 m air temperature, 2 m dewpoint temperature and 10 m wind components were obtained from the ERA5-Land reanalysis of the European Centre for Medium-Range Weather Forecasts at 0.1° resolution (≈9–11 km at the latitude of Lahore). Relative humidity was derived from air and dewpoint temperature using the Magnus formula, and wind speed was computed from the zonal (u) and meridional (v) wind components. Monthly precipitation was obtained from the Climate Hazards Group InfraRed Precipitation with Station data (CHIRPS). Monthly values were aggregated to winter (December–February, DJF), spring (March–May, MAM), summer/monsoon (June–August, JJA) and autumn (September–November, SON).

2.2.3 Socioeconomic Data and Spatial Sampling

Built-up area, road density and population were used as indicators of urban growth, infrastructure and human activity (Seto et al. 2012; Liu et al. 2020; Angel 2023). Land use was mapped from multi-temporal Landsat imagery (Seto et al. 2011; Naab et al. 2013; Chai and Li 2016; Naikoo et al. 2020; Shah et al. 2022) and classified into built-up, cultivated (green) and barren land using unsupervised classification in ArcGIS (Duda and Canty 2002). Road networks were derived from OpenStreetMap and digitized for each period against contemporaneous imagery, and gridded population was obtained from WorldPop, a product comparable to LandScan (Bhaduri et al. 2002; Bright et al. 2018).

2.2.4 Consistency of the $PM_{2.5}$ Dataset with Ground Observations

Ground observations cannot serve as a continuous reference for 2015–2024. Regulatory-grade monitoring in Lahore is limited to the United States (US) Consulate monitor, which published data from 2019 (Babar et al. 2024; IQAir n.d.) until March 2025 (Hasan and Myllyvirta 2025), a few Punjab Environmental Protection and Climate Change Department sites operated intermittently during 2019–2024, and an Urban Unit monitor at Township operating since 2021 (Babar et al. 2024). Real-time aggregators republish these monitors, and their historical data are unvalidated and

not intended for formal comparison (World Air Quality Index Project n.d.); they were therefore not used.

Because continuous ground monitoring is not available for the full study period, the satellite-derived dataset was compared with the limited published monitor data for Lahore in three ways: the seasonal pattern, annual levels and winter peaks (Table 1).

First, both the satellite data and the ground monitors show the same seasonal cycle, with the highest concentrations in winter and the lowest in the monsoon. Averaged over 2015–2024, the satellite data give city-wide means of about 97 µg/m³ in winter and 40 µg/m³ in the monsoon, a winter-to-monsoon ratio of about 2.4. The corresponding ratios at the ground monitors were about 2.7 at Township in 2022 (192.7 vs 72.3 µg/m³) and about 3.6 at the US Consulate in 2020 (166.3 vs 45.7 µg/m³) (Babar et al. 2024). The satellite data therefore capture the seasonal contrast, although less strongly than the US Consulate monitor.

Second, the satellite city-wide annual mean for 2022–2023 (about 71 µg/m³) is about 70–75% of the annual means of 97–100 µg/m³ reported for Lahore from ground monitoring in those years (Babar et al. 2024).

Third, in the same years as the monitor records, the highest winter values in central Lahore in the satellite data (about 125–132 µg/m³ in 2020 and 145–151 µg/m³ in 2022; Fig. 4) are about 75–80% of the winter means at the US Consulate and Township monitors.

Overall, the satellite data reproduce the seasonal pattern observed at the ground stations but underestimate absolute concentrations by roughly 20–30%. Such an underestimate is expected because each satellite value is a monthly average over a 1 km grid cell, whereas a ground monitor measures at a single point that is often close to local sources such as traffic (SatPM n.d.). Because the comparison uses different years and locations, it indicates broad consistency rather than formal validation. Because the socioeconomic model uses standardized $PM_{2.5}$, a constant additive or multiplicative bias does not affect its coefficients; a bias that varies with season or with a predictor (for example, relative humidity) could, however, affect the climatic coefficients. The dataset was therefore considered suitable for the relative spatiotemporal analysis undertaken here, and the coefficients are interpreted as relative associations with the satellite-derived $PM_{2.5}$ field.

Table 1 Comparison of the satellite-derived $PM_{2.5}$ dataset (this study) with published ground-monitor data for Lahore (Babar et al. 2024)

Comparison	Satellite (this study)	Ground monitor	Satellite as % of monitor
Winter-to-monsoon ratio	2.4 (2015–2024 average)	2.7 (Township, 2022); 3.6 (US Consulate, 2020)	—
Annual mean, 2022–2023	≈71 µg/m³ (city-wide)	97–100 µg/m³	≈70–75%
Winter peak, 2020	125–132 µg/m³ (central city)	166.3 µg/m³ (US Consulate)	≈75–79%
Winter peak, 2022	145–151 µg/m³ (central city)	192.7 µg/m³ (Township)	≈75–78%

2.3 Geographically and Temporally Weighted Regression Model

GTWR extends geographically weighted regression by estimating a separate set of coefficients for each location and time, weighting neighbouring observations by their proximity in space and time (Huang et al. 2010):

$$Y_i = \beta_0(u_i, v_i, t_i) + \sum_{k=1}^{p} \beta_k(u_i, v_i, t_i) X_{ik} + \varepsilon_i \quad (1)$$

where Y_i is $PM_{2.5}$ for observation i, X_{ik} is the kth of p predictors, (u_i, v_i) and t_i are the location and time of observation i, ε_i is the error term, and the local coefficients are estimated by weighted least squares:

$$\hat{\beta}(u_i, v_i, t_i) = [X^{\mathrm{T}} W(u_i, v_i, t_i) X]^{-1} X^{\mathrm{T}} W(u_i, v_i, t_i) Y \quad (2)$$

The weight matrix is the product of a spatial and a temporal Gaussian kernel:

$$W(u_i, v_i, t_i) = \mathrm{diag}\left(W_{ij}^{\mathrm{ST}}\right), \qquad W_{ij}^{\mathrm{ST}} = W_{ij}^{\mathrm{S}} \times W_{ij}^{\mathrm{T}} \quad (3)$$

$$W_{ij}^{\mathrm{S}} = \exp\left(-\frac{\left(d_{ij}^{\mathrm{S}}\right)^2}{h_{\mathrm{S}}^2}\right), \qquad \left(d_{ij}^{\mathrm{S}}\right)^2 = \left(u_i - u_j\right)^2 + \left(v_i - v_j\right)^2 \quad (4)$$

$$W_{ij}^{\mathrm{T}} = \exp\left(-\frac{\left(d_{ij}^{\mathrm{T}}\right)^2}{h_{\mathrm{T}}^2}\right), \qquad \left(d_{ij}^{\mathrm{T}}\right)^2 = \left(t_i - t_j\right)^2 \quad (5)$$

where d_{ij}^{S} is the Euclidean distance (m) between locations i and j, d_{ij}^{T} is their separation in time (season index for the climatic model and year index for the socioeconomic model), and h_{S} and h_{T} are the spatial and temporal bandwidths. Because both kernels are Gaussian, their product is equivalent to a single kernel of the space-time distance $\left[\left(d_{ij}^{\mathrm{S}}\right)^2 + \tau\left(d_{ij}^{\mathrm{T}}\right)^2\right]^{1/2}$, where $\tau = h_{\mathrm{S}}^2 / h_{\mathrm{T}}^2$ is the spatio-temporal scale parameter (Huang et al. 2010).

Two GTWR models were fitted independently (Table 2). The climatic model related seasonal $PM_{2.5}$ to temperature, relative humidity, rainfall and wind speed on a regular 7 × 5 grid of 35 points (1,400 point-seasons). Because ERA5-Land (≈9–11 km) resolves only regional, synoptic-scale gradients, the climatic model used these 35 grid points with an adaptive bandwidth of 53 nearest neighbours (space–time observations). The socioeconomic model related annual $PM_{2.5}$ to built-up area and road density (both log-transformed) and population at 571 urban locations (5,710 point-years). All variables in this model were standardized, so each local coefficient (b_z) is the change in $PM_{2.5}$, in standard deviations, per standard-deviation increase in the predictor, holding the other predictors constant. A single combined model was not feasible because the two sets of inputs differ in spatial resolution and temporal structure. Local significance was assessed with the local t-statistic ($t = \hat{\beta}_k / \text{local standard error}$) against the two-tailed critical value of 1.96 (5% level), and only coefficients significant at the 5% level are reported and used for the shaded map surfaces. In the seasonal maps (Fig. 5), the value at each grid point is the mean of its significant coefficients over 2015–2024.

Table 2 Final geographically and temporally weighted regression (GTWR) model specifications for the climatic and socioeconomic models reported in Section 3

Parameter	Climatic GTWR model	Socioeconomic GTWR model
Predictors	Temperature, relative humidity, rainfall, wind speed	Built-up area (BA, log), road density (RD, log), population (Pop)
Kernel	Gaussian	Gaussian
Bandwidth type	Adaptive (nearest neighbours)	Fixed
Bandwidth	53 nearest neighbours	2,140.3 m
Spatio-temporal scale (τ)	1.7	3.8
Locations	35 (7×5 regular grid)	571 unique urban locations
Temporal resolution	Seasonal (DJF, MAM, JJA, SON)	Annual
N (point-observations)	1,400 point-seasons	5,710 point-years
Significance threshold	$\|t\| \geq 1.96$ (5% level)	$\|t\| \geq 1.96$ (5% level)
R^2	0.894	0.562
AICc / BIC	9,869.1/ 9,953.2	11,528.0 / 11,720.4

AICc, corrected Akaike information criterion; BIC, Bayesian information criterion; BA, built-up area; RD, road density; Pop, population; DJF, December–February; MAM, March–May; JJA, June–August; SON, September–November

3. Results

3.1 Spatiotemporal Variation in $PM_{2.5}$

Annual mean $PM_{2.5}$ ranged from 62.9 µg/m³ (2020) to 74.5 µg/m³ (2021), reflecting interannual variability with peaks in 2016, 2018 and 2021 (Fig. 2). The 2020 minimum coincides with year-to-year meteorological variation and with the COVID-19 lockdowns in Pakistan from late March 2020 (Mehmood et al. 2021a). The fitted linear trend over the decade was 0.355 µg/m³ per year, an increase of about 3.2 µg/m³ (4.7%) between 2015 and 2024, and annual levels remained well above the World Health Organization (WHO) Interim Target 1 of 35 µg/m³ throughout.

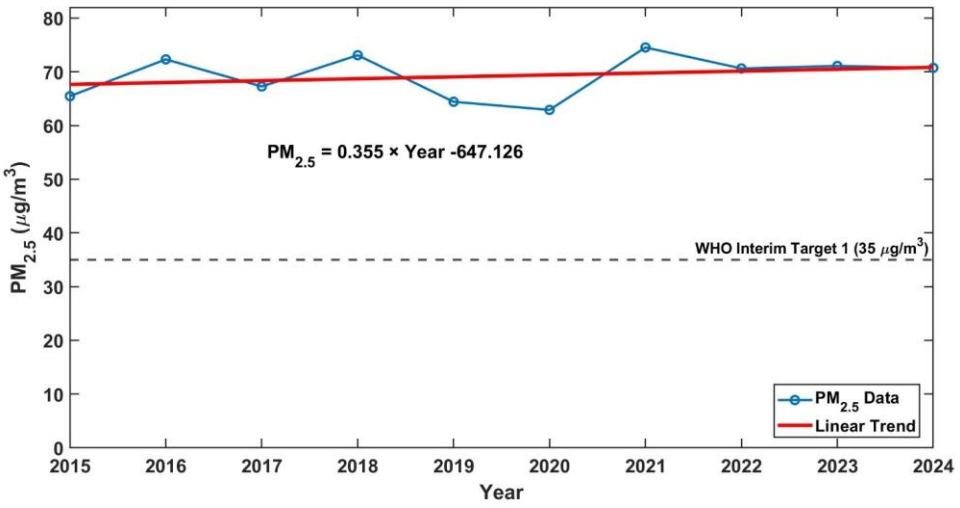


Fig. 2 Temporal trend and variation of the annual average $PM_{2.5}$ concentrations (µg/m³) in Lahore from 2015 to 2024, with the fitted linear trend; the dashed line marks the World Health Organization (WHO) Interim Target 1 (35 µg/m³)

In 2015–2017, concentrations were highest (about 70–79 µg/m³) in the central towns (Ravi, Shalimar, Data Ganj Bakhsh, Samanabad, Gulberg and Aziz Bhatti) and lower (about 52–67 µg/m³) in Wagah and parts of Iqbal and Nishtar (Fig. 3). From 2018, elevated concentrations spread southward toward Nishtar and Wagah and later westward toward Iqbal; by 2021–2024, most towns exceeded 70 µg/m³, and central areas reached the highest mapped class (79–90 µg/m³).

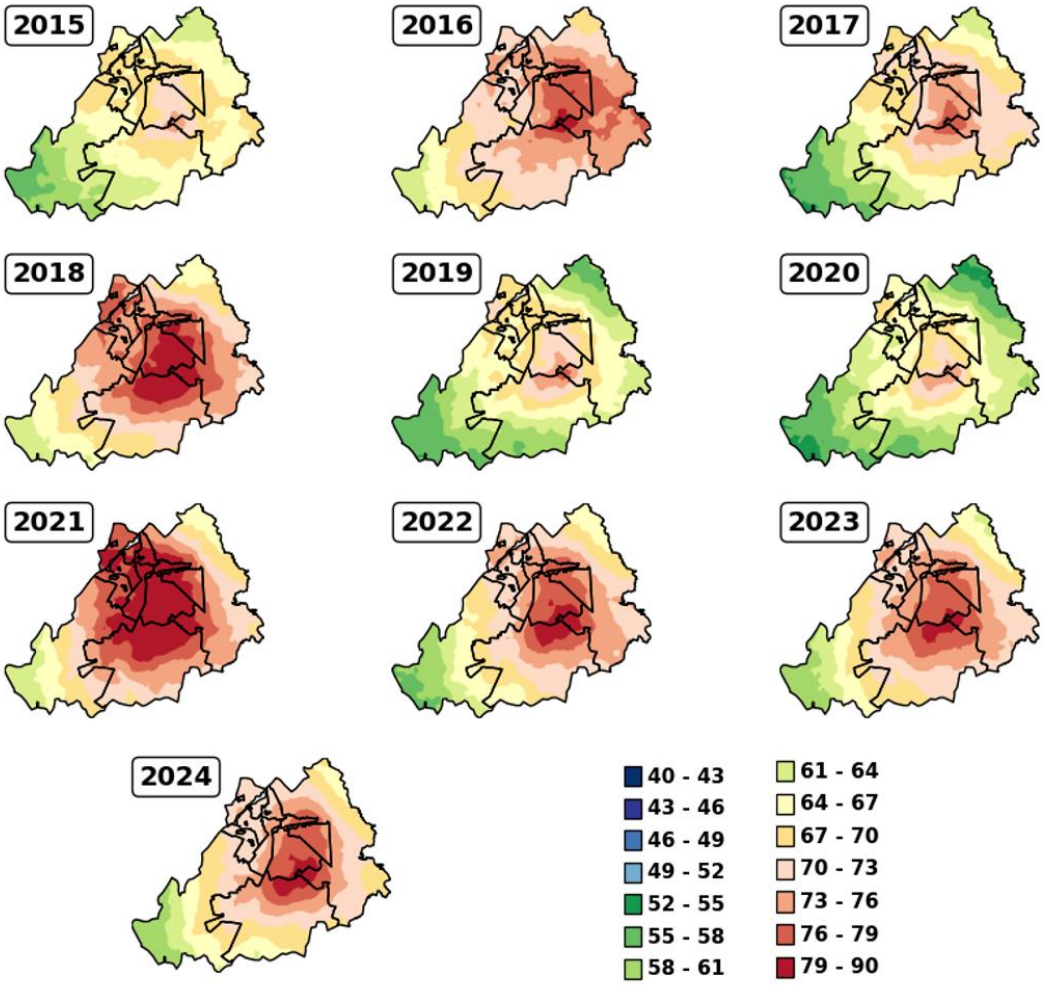


Fig. 3 Annual $PM_{2.5}$ concentrations (µg/m³) in Lahore, 2015–2024

Winter (DJF) concentrations were substantially higher than annual means (Fig. 4). Central areas already exceeded about 110 µg/m³ in 2015–2017; from 2020 onward, large parts of the city exceeded 100 µg/m³, and in 2021–2024 central peaks reached about 125–151 µg/m³, with peripheral areas typically at about 86–105 µg/m³. Averaged over 2015–2024, city-wide mean $PM_{2.5}$ was about 97 µg/m³ in winter and 40 µg/m³ in the monsoon (JJA).

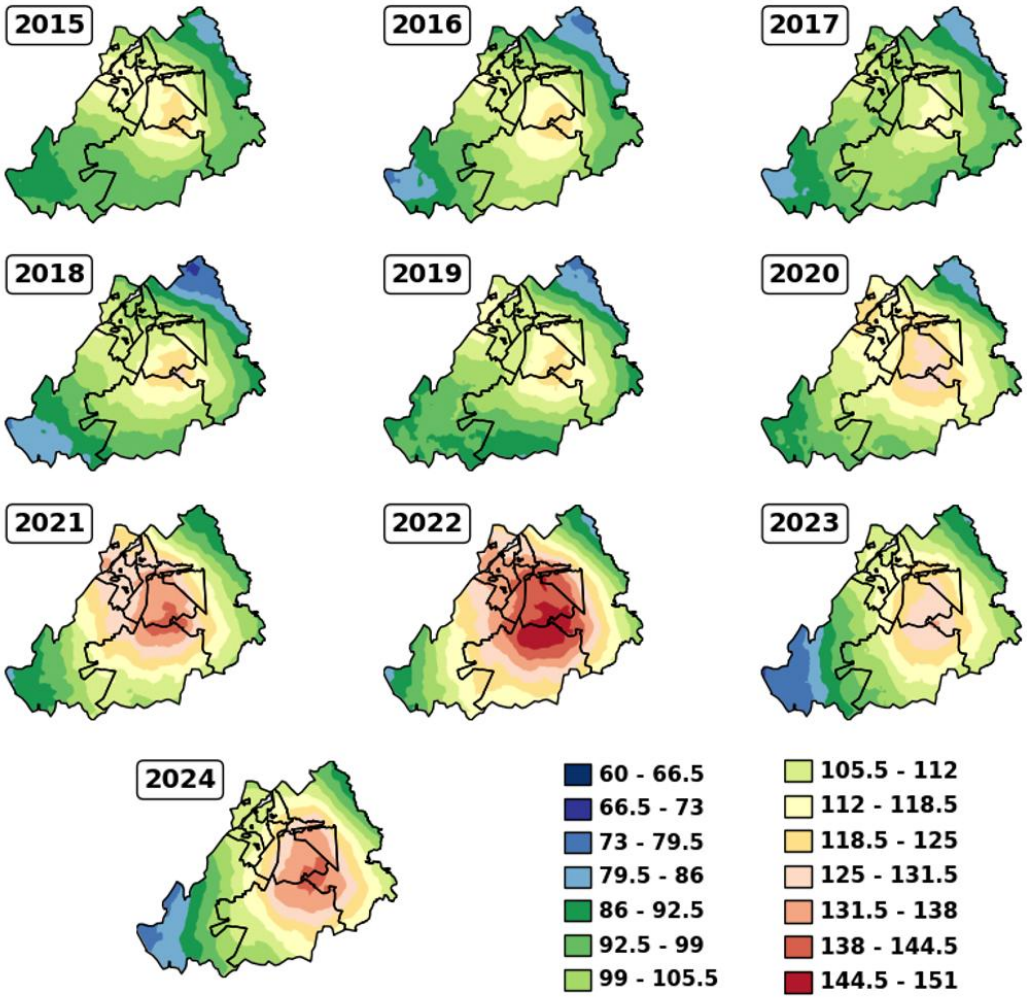


Fig. 4 Winter (December–February) $PM_{2.5}$ concentrations (μg/m³) in Lahore, 2015–2024

3.2 Climatic Factors and $PM_{2.5}$

The results below are from the final climatic model (Table 2; $R^2 = 0.894$). Seasonal maps of significant local coefficients are shown in Fig. 5.

3.2.1 Relative Humidity

Relative humidity was positively associated with $PM_{2.5}$ estimates in each season. Mean coefficients were highest in winter and summer (both ≈1.48), lowest in spring (≈1.40) and intermediate in autumn (≈1.45). The strongest effects were centred on the central-southern Model Town/Township/Iqbal Town/Johar Town belt (≈74.2–74.3°E, 31.4–31.5°N) and weakened toward the eastern rural fringe near Burki and the Wagah border (≈74.5–74.6°E) (Fig. 5a).

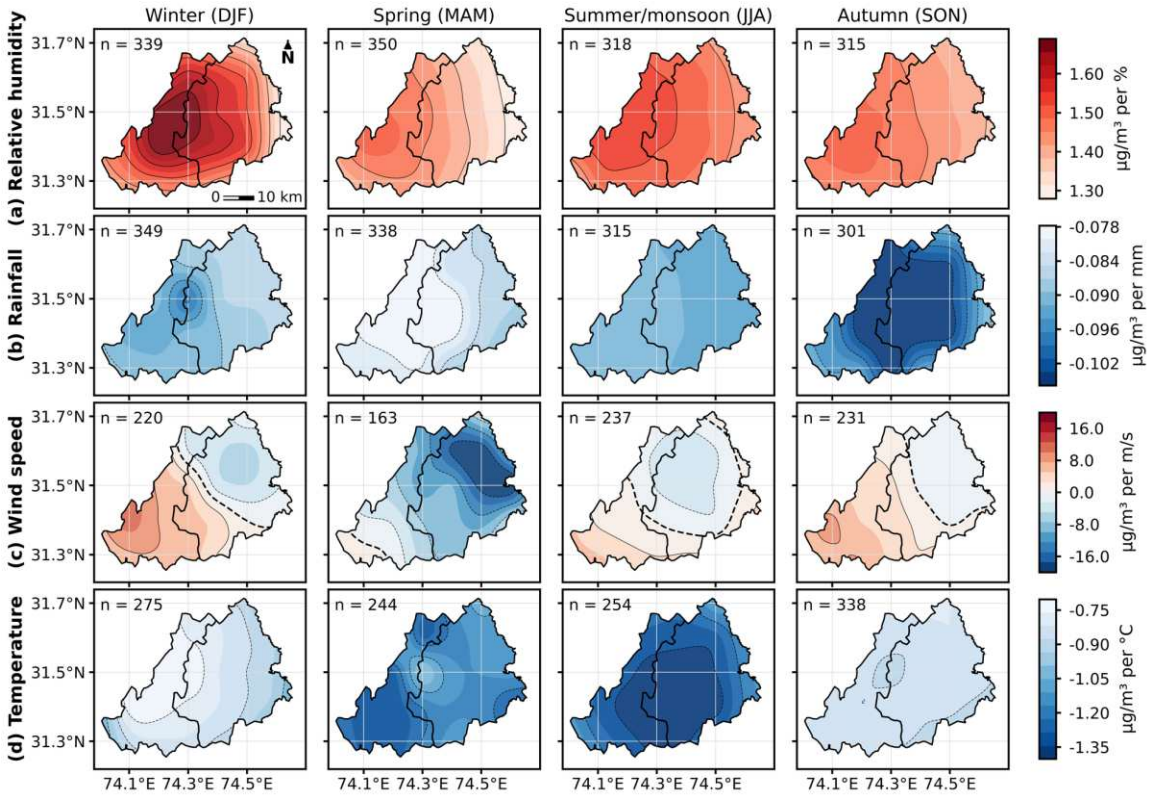


Fig. 5 Local geographically and temporally weighted regression (GTWR) coefficients of (a) relative humidity (µg/m³ per %), (b) rainfall (µg/m³ per mm), (c) wind speed (µg/m³ per m/s) and (d) temperature (µg/m³ per °C) on $PM_{2.5}$ by season: winter (December–February, DJF), spring (March–May, MAM), summer/monsoon (June–August, JJA) and autumn (September–November, SON). Coefficients are significant at 5% level; values at each grid point are means of the significant coefficients over 2015–2024, interpolated between grid points and clipped to the Lahore district boundary, and n is the number of significant coefficients out of 350 (35 grid points × 10 years) in each season. Each variable has a colour scale shared across seasons; for wind speed, the diverging scale is centred on zero and the dashed line marks the zero contour. Boundaries of the former Lahore City and Lahore Cantonment tehsils from geoBoundaries

3.2.2 Rainfall

Rainfall was negatively associated with $PM_{2.5}$ estimates in each season. The effect was strongest in autumn (SON, mean ≈ −0.098), weakest in spring (MAM, ≈ −0.082) and intermediate in winter (≈ −0.089) and summer (≈ −0.092). The strongest effects occurred in central Gulberg (≈74.3°E, 31.5°N) and the Defence Housing Authority (DHA)/Cantonment belt (≈74.5°E, 31.4°N), and the weakest along the northern edge near Shahdara and the Ravi riverbank (≈31.7°N) and the western edge (≈74.0–74.1°E) (Fig. 5b).

3.2.3 Wind Speed

Wind speed was the only climatic variable whose mean local coefficient changed sign across the city. Coefficients were negative in the north-east, around Shalimar, Baghbanpura, Harbanspura and the GT Road corridor toward Batapur (≈74.4–74.5°E, 31.55–31.65°N), and positive in the west, around Raiwind Road/Thokar Niaz Baig and the western outskirts (≈74.0–74.2°E) (Fig. 5c). This west-positive/north-east-negative pattern was present in winter, summer and autumn, although in summer the negative zone shifted to a broader central-eastern area. Spring differed: the positive

signal was confined to a narrow strip at the western edge, while the eastern two-thirds of the city was strongly negative, with a larger mean magnitude (≈ −6.3) than in any other season.

3.2.4 Temperature

Temperature coefficients were predominantly negative and significant in every season. The mean magnitude was largest in summer (JJA, ≈ −1.25) and spring (MAM, ≈ −1.20) and smaller in winter and autumn (≈ −0.86 and −0.84, respectively). The weakest effects occurred over the central Iqbal Town/Model Town cluster and the edge of the old city (≈74.1–74.3°E, 31.4–31.6°N), a pattern most pronounced in winter and visible in spring only at two central points (≈74.2°E, 31.6°N and 74.3°E, 31.5°N), and the strongest toward the eastern and south-eastern periphery of the district near the outer phases of DHA (≈74.5–74.6°E) (Fig. 5d).

3.3 Socioeconomic Factors and $PM_{2.5}$

3.3.1 Built-up Area

All significant built-up area coefficients were positive. The strongest effects formed a belt across Raiwind Tehsil on the southern periphery: the highest coefficient ($b_z = 0.312$, $t = 5.60$) was near Raiwind town, with further peaks along Sundar Road and Chah Jo Wala ($b_z = 0.307 - 0.310$, $t = 5.6 - 5.8$) and in Ashrafi Town near Rohi Nala Road ($b_z = 0.300$, $t = 5.66$), all within a few kilometres of the Sundar Industrial Estate. A smaller secondary cluster occurred in the central-eastern part of the city (≈74.37–74.40°E, 31.45–31.49°N; $b_z \approx 0.26 - 0.29$) (Fig. 6a).

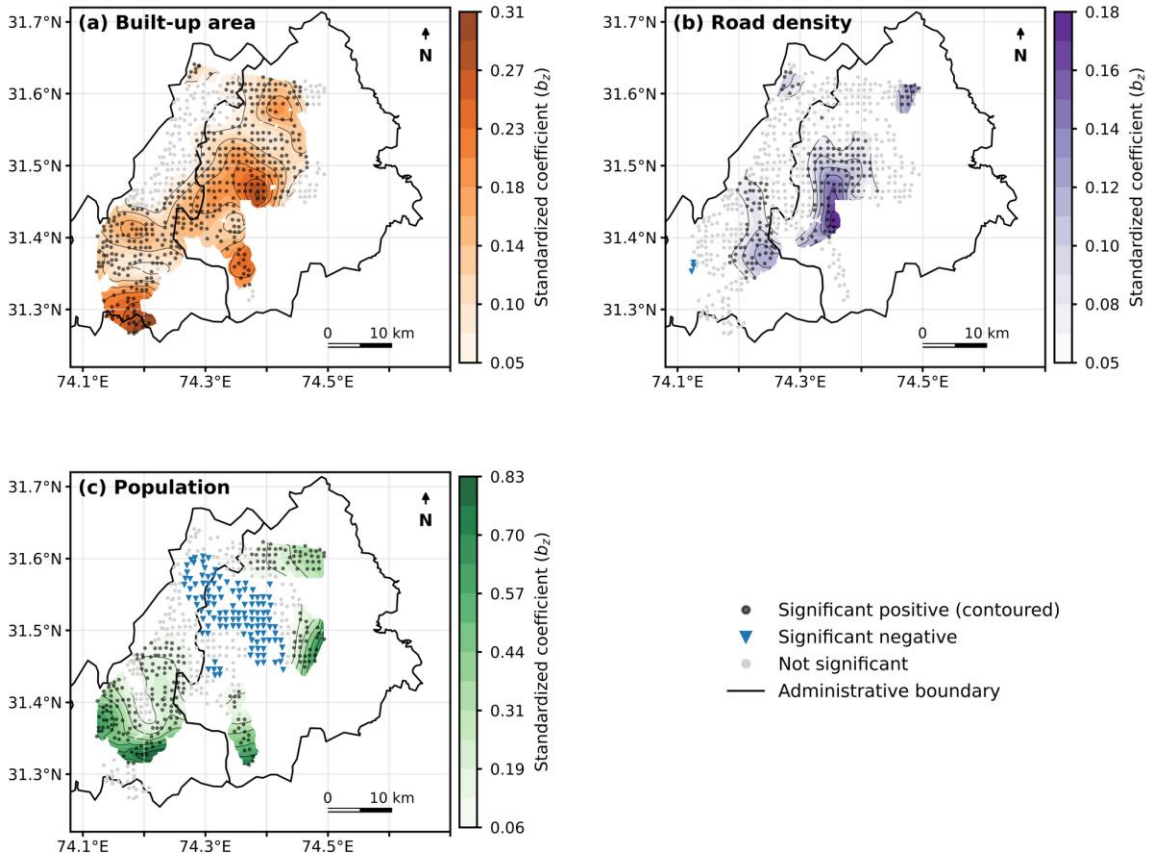


Fig. 6 Local standardized effects of (a) built-up area, (b) road density and (c) population on $PM_{2.5}$ at the 5% significance level ($|t| \geq 1.96$), from the socioeconomic geographically and temporally weighted regression model. Of 571 locations, built-up area had 417 significant positive, 0 significant negative and 154 non-significant coefficients; road density 163, 3 and 405; and population 234, 117 and 220. Surfaces are interpolated from the significant positive coefficients only and shown within about 1.5 km of them; blue triangles mark significant negative and grey dots non-significant coefficients. Values are highest in Raiwind Tehsil near the Sundar Industrial Estate (a), around Youhanabad, Model Town Tehsil (b), and on the urbanizing southern/south-western fringe near Jati Umra and Badhoke (c). Boundaries of the former Lahore City and Lahore Cantonment tehsils from geoBoundaries; tehsil names in the text follow the current administrative division

3.3.2 Road Density

Of the significant road-density coefficients, 98.2% were positive. The effect was more spatially concentrated than that of built-up area, with the highest values ($b_z = 0.150 - 0.178$, $t = 2.2 - 3.1$) around Youhanabad in Model Town Tehsil and in the adjacent Green Cap Housing Scheme and Ghawala Colony (Fig. 6b).

3.3.3 Population

Population had the largest positive coefficients of the three factors (mean of the significant positive coefficients at the 5% level: $b_z = 0.290$, compared with 0.141 for built-up area and 0.091 for road density), although a substantial minority of its significant coefficients (117 of 351) were negative (shown as triangles in Fig. 6c). The strongest positive effects ($b_z = 0.68 - 0.83$, $t = 3.5 - 5.9$, $p < 0.01$) were located on the southern and south-western urbanizing fringe around Jati Umra and Badhoke (Raiwind Tehsil), near Bhaiwala (Lahore Cantonment Tehsil) and at the eastern edge of the study area (≈74.49°E, 31.49°N) (Fig. 6c).

Across Figs. 6a–c, significant positive coefficients were generally larger toward the outer, southern and south-western parts of the study area and smaller in the older central and northern parts of the city.

4. Discussion

4.1 Climatic Factors and $PM_{2.5}$

The climatic results are consistent with known physical mechanisms. The positive humidity effect reflects hygroscopic growth of secondary sulphate, nitrate and organic aerosols, aqueous-phase secondary aerosol formation, and the association of humid air with the shallow, stable boundary layers and inversions that underlie Lahore's winter fog and smog episodes (Biswas et al. 2008). The effect was strongest in the dense central-southern belt, where the most particulate mass is available for water uptake, indicating that humidity amplifies existing pollution rather than creating it. The strong summer effect, despite the lowest $PM_{2.5}$ of the year, suggests that hygroscopic growth persists during the monsoon but is outweighed by wet removal.

Rainfall removes particles through in-cloud and below-cloud scavenging, suppresses the resuspension of road and construction dust, and accompanies monsoon ventilation. Its cleansing effect was largest in the most polluted, high-traffic areas, where more particulate mass is available for removal. The seasonal ordering is consistent with diminishing returns: frequent monsoon rain leaves little accumulated $PM_{2.5}$ between events, whereas the less frequent autumn rain follows a

period of rapid accumulation after monsoon withdrawal. The negative temperature effect reflects convective deepening of the boundary layer and the co-occurrence of warm, wet and well-ventilated conditions during the monsoon. Its weakness in the central part of the city, especially in winter, may reflect persistent inversions that limit vertical mixing. An urban heat-island effect cannot be assessed with these data because ERA5-Land does not explicitly represent the urban canopy.

The sign reversal of wind speed is the clearest evidence of spatial non-stationarity. In the open north-eastern Ravi/GT Road corridor, stronger wind dilutes local emissions, whereas the positive effect in the west may indicate transport: the western and south-western edge of the city borders the Punjab rice–wheat belt, and stronger winds may deliver more regionally transported crop-residue smoke and dust. Because wind speed carries no directional information, this transport interpretation remains a hypothesis, and edge effects and peri-urban sources such as brick kilns cannot be excluded. A global model would average these opposing effects into a weak and misleading city-wide estimate. The weak western signal in spring is consistent with the seasonality of crop-residue burning, which peaks after the autumn rice harvest, while pre-monsoon winds and dust storms leave wind with a mainly ventilating role. These findings add a spatially explicit meteorological dimension to earlier Lahore studies that identified transport, industry, biomass burning and transboundary pollution as the main sources (Aziz and Bajwa 2007, 2008; Ali and Athar 2010; Khanum et al. 2017; Bilal et al. 2022).

4.2 Socioeconomic Factors and the Peripheral Pattern

The larger socioeconomic coefficients on the periphery (Figs. 6a–c) have two substantive explanations. First, the coefficients are standardized marginal effects, and additional built-up area, roads or residents add less new emitting activity where these are already saturated, as in the mature central city; the log form of built-up area and road density is consistent with such diminishing returns. On the rapidly urbanizing fringe, the same increment represents genuinely new sources: construction and paving dust, unpaved-road dust, industrial and construction-material activity around the Sundar Industrial Estate, and solid-fuel and generator use where grid power and public transport are limited. Population there grows fastest in relative terms, largely through unplanned conversion of agricultural land, even though absolute densities remain below those of the old city. Second, the south-western fringe may coincide with the main entry route of regionally transported smoke (Section 4.1), so growth-related emissions and imported pollution may reinforce each other.

The road-density hotspot around Youhanabad reflects a dense residential area with narrow streets, heavy small-scale commercial and workshop traffic and limited arterial capacity, where road density acts as a proxy for stop-and-go traffic and roadside emissions rather than free-flowing arterial traffic. These patterns should be read with care: coefficients near the study-area boundary are estimated from one-sided neighbourhoods, local collinearity can blur separate effects in the dense core, and the largest values in Fig. 6c lie along the outer boundary. The maps show where additional growth is associated with the largest $PM_{2.5}$ increase per standardized unit; they do not imply that the core is cleaner, because the highest absolute concentrations remained in central Lahore (Section 3.1).

The significant negative population coefficients (117 of 571 locations), concentrated in the central and northern parts of the city (≈74.27–74.43°E, 31.44–31.60°N), do not imply that more residents reduce $PM_{2.5}$. Each coefficient is a partial effect estimated while holding built-up area and road density constant, and in the dense core these three variables are strongly correlated; WorldPop population estimates are themselves modelled partly from settlement and road covariates. At these locations, $PM_{2.5}$ was highest (mean 73.5 μg/m³) and the built-up area and road-density coefficients were most often positive and significant (road density at 46% of these locations, compared with 18–30% elsewhere), indicating that the built-environment variables absorb most of the association. Conditional on the built environment, a larger residential (night-time) population may indicate predominantly residential land use, with less commercial, transport and workshop activity, which are the main sources of daytime emissions. In addition, population in the core changes little over time and space, so its local slope is weakly identified. Established neighbourhoods with piped gas and grid electricity may also rely less on solid fuels and generators. These negative coefficients should therefore be read as a statistical consequence of collinearity and land-use mix rather than as a protective effect of population.

4.3 Compound Hotspots and a Seasonal Climatic Overlay

Two areas combine structural and climatic drivers. On the south-western periphery (Raiwind Tehsil, including Sundar Road, Chah Jo Wala, Ashrafi Town, Jati Umra and Badhoke), the highest built-up area and population coefficients coincide with the positive wind-speed effect, which may be transport-related. This area generates a rising local emission baseline and may also receive imported smoke, which could compound $PM_{2.5}$ during the post-monsoon and winter burning season, whereas in spring the wind-speed association there is weak. In central-southern Lahore, the Youhanabad/Model Town road-density hotspot lies at the eastern margin of the belt of strongest humidity effects, so traffic emissions there are most likely to be amplified and trapped under humid, calm and inverted winter conditions.

Taken together, the two models suggest that $PM_{2.5}$ at a given place and time behaves approximately as a structural baseline, set by built-up area, road density and population, modulated by a strongly seasonal climatic overlay, as reflected in the more than two-fold difference between winter (≈97 μg/m³) and monsoon (≈40 μg/m³) means. Locations with a high structural baseline are therefore expected to experience their worst absolute $PM_{2.5}$ in humid, rain-free and calm winter months, consistent with the intensifying and expanding winter pollution in Fig. 4. This pattern is set against Lahore's rapid growth: improvements in transport, services and commercial development have attracted migration and outward expansion (Conrad and Seitz 1994; Shirazi and Kazmi 2014; Ghafoor et al. 2022), increasing population, traffic, energy use and industrial activity on the urban fringe. Because the two models were estimated independently at different resolutions, these correspondences are descriptive geographic overlays rather than statistically estimated interactions.

4.4 Implications for Urban Planning and Regional Adaptation

The results point to spatially and seasonally differentiated planning rather than uniform city-wide measures, and identify where urban growth and climate act together across Lahore and its hinterland. Three priority areas emerge. (i) On the south-western fringe in Raiwind Tehsil, around the Sundar Industrial Estate and Jati Umra/Badhoke, where built-up area and population have their largest associations with $PM_{2.5}$, the pace and form of peri-urban expansion and industrial siting

should be guided through land-use planning, and the contribution of seasonal crop-residue burning should be addressed through cross-jurisdictional cooperation within the Indo-Gangetic Plain. (ii) In the Youhanabad/Model Town corridor, where road density has its strongest association with $PM_{2.5}$ at the eastern margin of the belt of strongest humidity effects, transport and land-use planning should aim to reduce congestion and roadside exposure, particularly during humid, low-wind winter conditions. (iii) The open north-eastern Shalimar/Ravi/GT Road corridor, where stronger winds were associated with lower $PM_{2.5}$, appears to act as a natural ventilation pathway and should be considered in zoning decisions that limit further built-up encroachment. At the scale of the urban region, the development plan could incorporate these spatial and seasonal patterns, existing seasonal measures such as winter burning restrictions could be evaluated against them, urban green space should be protected and expanded (Khan et al. 2022), and meteorologically informed early-warning systems could help residents and institutions adapt during high-risk winter periods.

These patterns are likely to be relevant beyond Lahore. Many cities of the Indo-Gangetic Plain combine rapid peri-urban expansion onto agricultural land, winter stagnation and trans-boundary influences from seasonal crop-residue burning. The spatially explicit framework used here relies only on openly available satellite, reanalysis and remote-sensing data and can therefore be applied to other data-limited urban regions to identify where, and in which seasons, urban growth and climate act together.

5. Conclusions

The main strength of this study is the integration of a decade of gridded $PM_{2.5}$, reanalysis climate and socioeconomic data within a spatially and temporally varying framework that is transferable to other data-limited cities. The limitation of this study is the climatic and socioeconomic variables could not be combined in a single GTWR model because of their different spatial resolution and temporal structure; a jointly estimated model on a common grid would allow the compound effects described in Section 4.3 to be tested formally. $PM_{2.5}$ in Lahore remained far above WHO targets during 2015–2024, increased modestly and spread from the urban core toward the periphery, with the highest concentrations in winter. Relative humidity and rainfall had consistently positive and negative effects, respectively, across the city, temperature was mainly dispersive, and wind speed had a dual, location-dependent role: dispersive in the open north-east but positive, and possibly transport-related, in the west. Built-up area, road density and population were predominantly positive, spatially concentrated drivers, with the strongest effects on the rapidly urbanizing south-western periphery around Raiwind Tehsil and a traffic-related hotspot around Youhanabad. Socioeconomic factors therefore largely determine where $PM_{2.5}$ is generated, while climatic conditions govern its accumulation, transport and removal, and their overlap on the south-western fringe is likely to compound pollution. Effective mitigation in Lahore will require spatially and seasonally targeted interventions supported by meteorologically informed forecasting and early-warning systems.

Compliance with Ethical Standards

Funding: N/A.

Conflict of Interest: The authors declare that they have no conflict of interest.

Research involving Human Participants and/or Animals: This study used only publicly available, open-source secondary data: satellite-derived $PM_{2.5}$ estimates (ACAG V5.GL.06), ERA5-Land climate reanalysis and CHIRPS precipitation data, Landsat satellite imagery, WorldPop gridded population data, and OpenStreetMap road data. These are gridded or aggregated environmental and spatial datasets. No human participants, animals, personal data or identifiable information were involved, and ethics approval was therefore not required.

Informed consent: Not applicable.

CRediT Authorship Contribution Statement

Conceptualization: ZF, BU, ZA. Formal analysis and investigation (including interpretation of climate variables): SR, SN. Writing – review & editing: all authors. All authors read and approved the final manuscript.

Acknowledgements

We acknowledge the support provided for this study by the Environmental-Occupational Health & Climate Change section and the Epidemiology & Biostatistics section of the Department of Community Health Sciences of Aga Khan University, Pakistan.

Supplementary Data

No supplementary data are provided with this study.

Data Availability

All data used in this study are publicly available: ACAG V5.GL.06 $PM_{2.5}$ (https://wustl.app.box.com/v/ACAG-V5GL06-GWRPM25/folder/349056563741?page=1); ERA5-Land monthly means (https://cds.climate.copernicus.eu/datasets/reanalysis-era5-land-monthly-means); CHIRPS precipitation (https://data.chc.ucsb.edu/products/CHIRPS-2.0/global_monthly/netcdf/byYear/); Landsat imagery (United States Geological Survey (USGS) EarthExplorer, https://earthexplorer.usgs.gov/); WorldPop population (https://hub.worldpop.org/geodata/summary?id=78725); OpenStreetMap data for Pakistan

(https://download.geofabrik.de/asia/pakistan.html); and administrative boundaries used in Figures 5 and 6 (geoBoundaries, https://www.geoboundaries.org/).

References

Alexeeff SE, Liao NS, Liu X, Van Den Eeden SK, Sidney S (2021) Long-term PM2.5 exposure and risks of ischemic heart disease and stroke events: review and meta-analysis. J Am Heart Assoc 10:e016890. doi: 10.1161/JAHA.120.016890

Ali M, Athar M (2010) Impact of transport and industrial emissions on the ambient air quality of Lahore City, Pakistan. Environ Monit Assess 171:353–363. doi: 10.1007/s10661-009-1283-0

Angel S (2023) Urban expansion: theory, evidence and practice. Build Cities 4:124–138. doi: 10.5334/bc.348

Aziz A, Bajwa IU (2007) Minimizing human health effects of urban air pollution through quantification and control of motor vehicular carbon monoxide (CO) in Lahore. Environ Monit Assess 135:459–464. doi: 10.1007/s10661-007-9665-7

Aziz A, Bajwa IU (2008) Erroneous mass transit system and its tended relationship with motor vehicular air pollution (an integrated approach for reduction of urban air pollution in Lahore). Environ Monit Assess 137:25–33. doi: 10.1007/s10661-007-9717-z

Babar ZB, Kamil I, Latif MH (2024) Situational analysis of air quality in Lahore. WWF-Pakistan, Lahore. https://wwfasia.awsassets.panda.org/downloads/situational-analysis-of-air-quality-of-lahore_1_1.pdf. Accessed 20 October 2026

Bari MA, Kindzierski WB (2017) Characteristics of air quality and sources affecting fine particulate matter (PM2.5) levels in the City of Red Deer, Canada. Environ Pollut 221:367–376. doi: 10.1016/j.envpol.2016.11.087

Bhaduri B, Bright E, Coleman P, Dobson J (2002) LandScan: locating people is what matters. Geoinformatics 5:34–37

Bilal M, Hassan M, Tahir DBT, Iqbal MS, Shahid I (2022) Understanding the role of atmospheric circulations and dispersion of air pollution associated with extreme smog events over South Asian megacity. Environ Monit Assess 194:82. doi: 10.1007/s10661-021-09674-y

Biswas KF, Ghauri BM, Husain L (2008) Gaseous and aerosol pollutants during fog and clear episodes in South Asian urban atmosphere. Atmos Environ 42:7775–7785. https://www.sciencedirect.com/science/article/abs/pii/S1352231008004986

Bright EA, Rose AN, Urban ML, McKee J (2018) LandScan 2017 high-resolution global population dataset. Oak Ridge National Laboratory, Oak Ridge, TN

Chai B, Li P (2016) Urban expansion extraction and analysis using Landsat time series data – a case study of Tianjin. In: 2016 IEEE International Geoscience and Remote Sensing Symposium (IGARSS), Beijing, China. doi: 10.1109/IGARSS.2016.7730908

Chen J, Wang SJ, Zhou CS, Li M (2019) Does the path of technological progress matter in mitigating China's PM2.5 concentrations? Evidence from three urban agglomerations in China. Environ Pollut 254:113012. doi: 10.1016/j.envpol.2019.113012

554 Cheng Z, Li L, Liu J (2017) Identifying the spatial effects and driving factors of urban PM2.5
555 pollution in China. Ecol Indic 82:61–75.
556 https://linkinghub.elsevier.com/retrieve/pii/S1470160X17303850
557 Cohen AJ, Brauer M, Burnett R, Anderson HR, Frostad J, et al (2017) Estimates and 25-year
558 trends of the global burden of disease attributable to ambient air pollution: an analysis of data
559 from the Global Burden of Diseases Study 2015. Lancet 389:1907–1918. doi: 10.1016/S0140-
560 6736(17)30505-6
561 Conrad K, Seitz H (1994) The economic benefits of public infrastructure. Appl Econ 26:303–311.
562 doi: 10.1080/00036849400000077
563 Duda T, Canty M (2002) Unsupervised classification of satellite imagery: choosing a good
564 algorithm. Int J Remote Sens 23:2193–2212. doi: 10.1080/01431160110078467
565 Fernando HJS, Mammarella MC, Grandoni G, Fedele P, Di Marco R, et al (2012) Forecasting
566 PM10 in metropolitan areas: efficacy of neural networks. Environ Pollut 163:62–67. doi:
567 10.1016/j.envpol.2011.12.018
568 Ghafoor N, Mehr-un-Nisa, Akbar MR (2022) Socioeconomic determinants of migration in the
569 city of Lahore, Pakistan. J Knowl Econ 13:3029–3049. doi: 10.1007/s13132-021-00844-4
570 Gurjar BR, Butler TM, Lawrence MG, Lelieveld J (2008) Evaluation of emissions and air quality
571 in megacities. Atmos Environ 42:1593–1606. doi: 10.1016/j.atmosenv.2007.10.048
572 Hammer MS, van Donkelaar A, Bindle L, Sayer AM, Lee J, et al (2023) Assessment of the
573 impact of discontinuity in satellite instruments and retrievals on global PM2.5 estimates.
574 Remote Sens Environ 294:113624. doi: 10.1016/j.rse.2023.113624
575 Hamra GB, Guha N, Cohen A, Laden F, Raaschou-Nielsen O, et al (2014) Outdoor particulate
576 matter exposure and lung cancer: a systematic review and meta-analysis. Environ Health
577 Perspect 122:906–911. doi: 10.1289/ehp.1408092
578 Hasan K, Myllyvirta L (2025) U.S. embassy AQ data halt: ramped up government monitoring
579 could save hundreds of millions of dollars per city. Centre for Research on Energy and Clean
580 Air. https://energyandcleanair.org/us-embassy-aq-data-halt/. Accessed 20 October 2026
581 He J, Gong S, Yu Y, Yu L, Wu L, et al (2017) Air pollution characteristics and their relation to
582 meteorological conditions during 2014–2015 in major Chinese cities. Environ Pollut 223:484–
583 496. doi: 10.1016/j.envpol.2017.01.050
584 Huang B, Wu B, Barry M (2010) Geographically and temporally weighted regression for
585 modeling spatio-temporal variation in house prices. Int J Geogr Inf Sci 24:383–401. doi:
586 10.1080/13658810802672469
587 IQAir (n.d.) Lahore air quality index (AQI) and Pakistan air pollution.
588 https://www.iqair.com/us/pakistan/punjab/lahore. Accessed 20 October 2026
589 Khanum F, Chaudhry MN, Kumar P (2017) Characterization of five-year observation data of fine
590 particulate matter in the metropolitan area of Lahore. Air Qual Atmos Health 10:725–736. doi:
591 10.1007/s11869-017-0464-1

592 Lecoeur E, Seigneur C (2013) Dynamic evaluation of a multi-year model simulation of
593 particulate matter concentrations over Europe. Atmos Chem Phys 13:4319–4337. doi:
594 10.5194/acp-13-4319-2013

595 Liu L (2013) Geographic approaches to resolving environmental problems in search of the path to
596 sustainability: the case of polluting plant relocation in China. Appl Geogr 45:138–146.
597 https://www.sciencedirect.com/science/article/abs/pii/S0143622813002026

598 Liu Q, Wang S, Zhang W, Li J, Dong G (2019) The effect of natural and anthropogenic factors on
599 PM2.5: empirical evidence from Chinese cities with different income levels. Sci Total Environ
600 653:157–167. https://www.sciencedirect.com/science/article/abs/pii/S0048969718342670

601 Liu Q, Wu R, Zhang W, Li W, Wang S (2020) The varying driving forces of PM2.5
602 concentrations in Chinese cities: insights from a geographically and temporally weighted
603 regression model. Environ Int 145:106168. doi: 10.1016/j.envint.2020.106168

604 Luo K, Li G, Fang C, Sun S (2018) PM2.5 mitigation in China: socioeconomic determinants of
605 concentrations and differential control policies. J Environ Manage 213:47–55.
606 https://www.sciencedirect.com/science/article/abs/pii/S0301479718301518

607 Lyu W, Li Y, Guan D, Zhao H, Zhang Q, et al (2016) Driving forces of Chinese primary air
608 pollution emissions: an index decomposition analysis. J Clean Prod 133:136–144. doi:
609 10.1016/j.jclepro.2016.04.093

610 Megaritis AG, Fountoukis C, Charalampidis PE, Denier van der Gon HAC, Pilinis C, et al (2014)
611 Linking climate and air quality over Europe: effects of meteorology on PM2.5 concentrations.
612 Atmos Chem Phys 14:10283–10298. doi: 10.5194/acp-14-10283-2014

613 Mehmood K, Bao Y, Petropoulos GP, Abbas R, Abrar MM, et al (2021a) Investigating
614 connections between COVID-19 pandemic, air pollution and community interventions for
615 Pakistan employing geoinformation technologies. Chemosphere 272:129809. doi:
616 10.1016/j.chemosphere.2021.129809

617 Mehmood U, Azhar A, Qayyum F, Nawaz H, Tariq S, et al (2021b) Air pollution and
618 hospitalization in megacities: empirical evidence from Pakistan. Environ Sci Pollut Res
619 28:51384–51390. doi: 10.1007/s11356-021-14158-0

620 Molina MJ, Molina LT (2004) Megacities and atmospheric pollution. J Air Waste Manag Assoc
621 54:644–680. doi: 10.1080/10473289.2004.10470936

622 Murray CJL, Aravkin AY, Zheng P, Abbafati C, Abbas KM, et al (2020) Global burden of 87 risk
623 factors in 204 countries and territories, 1990–2019: a systematic analysis for the Global
624 Burden of Disease Study 2019. Lancet 396:1223–1249. doi: 10.1016/S0140-6736(20)30752-2

625 Naab FZ, Dinye RD, Kasanga RK (2013) Urbanisation and its impact on agricultural lands in
626 growing cities in developing countries: a case study of Tamale in Ghana. Mod Soc Sci J
627 2:256–287

628 Naikoo MW, Rihan M, Ishtiaque M, Shahfahad (2020) Analyses of land use land cover (LULC)
629 change and built-up expansion in the suburb of a metropolitan city: spatio-temporal analysis of
630 Delhi NCR using Landsat datasets. J Urban Manag 9:347–359.
631 https://www.sciencedirect.com/science/article/pii/S2226585620300637

Pakistan Bureau of Statistics (2017) Population Census 2017: district-wise results, Punjab (Table 3: area, population by sex, sex ratio, population density, urban proportion, household size and annual growth rate). Pakistan Bureau of Statistics, Islamabad. https://www.pbs.gov.pk/sites/default/files/population/2017/punjab_district_wise.pdf. Accessed 20 October 2026

Pakistan Bureau of Statistics (2023) Punjab census insight: 7th Population and Housing Census 2023. Pakistan Bureau of Statistics, Islamabad. https://www.pbs.gov.pk/sites/default/files/population/2023/material/punjab_insight.pdf. Accessed 20 October 2026

SatPM (n.d.) SatPM V5.GL.06: global estimates of ground-level fine particulate matter, 1998–2024. Washington University in St. Louis, St. Louis, MO. https://www.satpm.org/v5-gl-06. Accessed 20 October 2026

Seto KC, Fragkias M, Güneralp B, Reilly MK (2011) A meta-analysis of global urban land expansion. PLoS One 6:e23777. doi: 10.1371/journal.pone.0023777

Seto KC, Güneralp B, Hutyra LR (2012) Global forecasts of urban expansion to 2030 and direct impacts on biodiversity and carbon pools. Proc Natl Acad Sci USA 109:16083–16088. doi: 10.1073/pnas.1211658109

Shah A, Ali K, Nizami SM (2022) Spatio-temporal analysis of urban sprawl in Islamabad, Pakistan during 1979–2019, using remote sensing. GeoJournal 87:2935–2948. doi: 10.1007/s10708-021-10413-6

Shirazi SA, Kazmi SJH (2014) Analysis of population growth and urban development in Lahore-Pakistan using geospatial techniques: suggesting some future options. South Asian Stud 29:269–280. https://pu.edu.pk/images/journal/csas/PDF/20%20Safdar%20Shirazi_29_1.pdf

Siwek K, Osowski S (2012) Improving the accuracy of prediction of PM10 pollution by the wavelet transformation and an ensemble of neural predictors. Eng Appl Artif Intell 25:1246–1258. https://www.sciencedirect.com/science/article/abs/pii/S0952197611002119

Southerland VA, Brauer M, Mohegh A, Hammer MS, van Donkelaar A, et al (2022) Global urban temporal trends in fine particulate matter (PM2.5) and attributable health burdens: estimates from global datasets. Lancet Planet Health 6:e139–e146. doi: 10.1016/S2542-5196(21)00350-8

Sughis M, Nawrot TS, Ihsan-ul-Haque S, Amjad A, Nemery B (2012) Blood pressure and particulate air pollution in schoolchildren of Lahore, Pakistan. BMC Public Health 12:378. doi: 10.1186/1471-2458-12-378

Tahir N (2017) The size and growth of the economy of Lahore. Lahore Chamber of Commerce and Industry, Lahore. https://sdpi.org/assets/lib/uploads/The-Size-and-Growth-of-the-Economy-of-Lahore.pdf. Accessed 20 October 2026

UNEP (2021) Pollution action note – data you need to know. United Nations Environment Programme, Nairobi. https://www.unep.org/interactives/air-pollution-note/. Accessed 20 October 2026

United Nations (1992) United Nations Framework Convention on Climate Change. United Nations, New York. http://unfccc.int/resource/docs/convkp/conveng.pdf. Accessed 20 October 2026

United Nations (2018) The world's cities in 2018 – data booklet (ST/ESA/SER.A/417). Department of Economic and Social Affairs, Population Division, United Nations, New York. https://digitallibrary.un.org/record/3799524/files/the_worlds_cities_in_2018_data_booklet.pdf . Accessed 20 October 2026

van Donkelaar A, Martin RV, Brauer M, Hsu NC, Kahn RA, et al (2016) Global estimates of fine particulate matter using a combined geophysical-statistical method with information from satellites, models, and monitors. Environ Sci Technol 50:3762–3772. doi: 10.1021/acs.est.5b05833

van Donkelaar A, Hammer MS, Bindle L, Brauer M, Brook JR, et al (2021) Monthly global estimates of fine particulate matter and their uncertainty. Environ Sci Technol 55:15287–15300. doi: 10.1021/acs.est.1c05309

Vodonos A, Awad YA, Schwartz J (2018) The concentration-response between long-term PM2.5 exposure and mortality; a meta-regression approach. Environ Res 166:677–689. doi: 10.1016/j.envres.2018.06.021

Wang S, Zhou C, Wang Z, Feng K, Hubacek K (2017) The characteristics and drivers of fine particulate matter (PM2.5) distribution in China. J Clean Prod 142:1800–1809. doi: 10.1016/j.jclepro.2016.11.104

Wang X, Tian G, Yang D, Zhang W, Lu D, et al (2018) Responses of PM2.5 pollution to urbanization in China. Energy Policy 123:602–610. doi: 10.1016/j.enpol.2018.09.001

Wang Q, Kwan M-P, Zhou K, Fan J, Wang Y, et al (2019) The impacts of urbanization on fine particulate matter (PM2.5) concentrations: empirical evidence from 135 countries worldwide. Environ Pollut 247:989–998. doi: 10.1016/j.envpol.2019.01.086

Wang SJ, Gao S, Li SJ, Feng KS (2020) Strategizing the relation between urbanization and air pollution: empirical evidence from global countries. J Clean Prod 243:118615. doi: 10.1016/j.jclepro.2019.118615

World Air Quality Index Project (n.d.) Air quality historical data platform: terms of service and usage statement. https://aqicn.org/data-platform/register/. Accessed 20 October 2026

Zhan D, Kwan M-P, Zhang W, Yu X, Meng B, et al (2018) The driving factors of air quality index in China. J Clean Prod 197:1342–1351. doi: 10.1016/j.jclepro.2018.06.108